

The width difference in the $B-\bar{B}$ system at next-to-next-to-leading order of QCD

Marvin Gerlach,^{1,*} Ulrich Nierste,^{1,†} Vladyslav Shtabovenko,^{1,‡} and Matthias Steinhauser^{1,§}

¹*Institut für Theoretische Teilchenphysik, Karlsruhe Institute of Technology (KIT), 76128 Karlsruhe, Germany*

We extend the theoretical prediction for the width difference $\Delta\Gamma_q$ in the mixing of neutral B mesons in the Standard Model to next-to-next-to-leading order in α_s . To this aim we calculate three-loop diagrams with two $|\Delta B| = 1$ current-current operators analytically. In the matching between $|\Delta B| = 1$ and $|\Delta B| = 2$ effective theories we regularize the infrared divergences dimensionally and take into account all relevant evanescent operators. Further elements of the calculation are the two-loop renormalization matrix Z_{ij} for the $|\Delta B| = 2$ operators and the $\mathcal{O}(\alpha_s^2)$ corrections to the finite renormalization that ensures the $1/m_b$ suppression of the operator R_0 at two-loop order. Our theoretical prediction reads $\Delta\Gamma_s/\Delta M_s = (4.33 \pm 0.93) \cdot 10^{-3}$ if expressed in terms of the bottom mass in the $\overline{\text{MS}}$ scheme and $\Delta\Gamma_s/\Delta M_s = (4.20 \pm 0.95) \cdot 10^{-3}$ for the use of the potential-subtracted mass. While the controversy on $|V_{cb}|$ affects both $\Delta\Gamma_s$ and ΔM_s , the ratio $\Delta\Gamma_s/\Delta M_s$ is not affected by the uncertainty in $|V_{cb}|$.

Introduction. The weak interaction of the Standard Model (SM) permits transitions between a neutral B_q meson and its antiparticle \bar{B}_q , where $q = d$ or s . The corresponding transition amplitude is mediated by box diagrams with W bosons and up-type quarks u , c , or t on the internal lines. The time evolution of the two-state system ($|B_q\rangle, |\bar{B}_q\rangle$) is governed by two hermitian 2×2 matrices, the mass matrix M^q and the decay matrix Γ^q . By diagonalizing $M^q - i\Gamma^q/2$ one finds the mass eigenstates $|B_L^q\rangle$ and $|B_H^q\rangle$ expressed in terms of the flavour eigenstates $|B_q\rangle, |\bar{B}_q\rangle$. The mass eigenstates differ in their masses $M_{H,L}^q$ and decay widths $\Gamma_{H,L}^q$ with “L” and “H” denoting “light” and “heavy”. There are three observables, the mass and width differences $\Delta M_q = M_H^q - M_L^q$ and $\Delta\Gamma_s = \Gamma_L^q - \Gamma_H^q$ as well as the CP asymmetry in flavor-specific decays, a_{fs}^q . Experimentally, ΔM_q is read off from the $B_q-\bar{B}_q$ oscillation frequency, $\Delta\Gamma_q$ is found by measuring lifetimes in different decay modes, and a_{fs}^q is usually measured through the time-dependent CP asymmetry in semileptonic B_q decays. These observables are related to the off-diagonal elements of M^q and Γ^q as follows:

$$\Delta M_q \simeq 2|M_{12}^q|, \quad \frac{\Delta\Gamma_q}{\Delta M_q} = -\text{Re} \frac{\Gamma_{12}^q}{M_{12}^q}, \quad a_{\text{fs}}^q = \text{Im} \frac{\Gamma_{12}^q}{M_{12}^q}, \quad (1)$$

with $|\Delta\Gamma_q| \simeq 2|\Gamma_{12}^q|$. M_{12}^q is sensitive to new physics mediated by particles with masses well beyond 100 TeV. On the contrary, Γ_{12}^q probes effects of light new particles with feeble couplings to quarks (see e.g. Refs. [1, 2]). While this is one motivation for a more precise SM prediction of Γ_{12}^q , a better knowledge of Γ_{12}^q will also help to reveal new physics in M_{12}^q : Inclusive and exclusive semileptonic B decays give different values for the element $|V_{cb}|$ of the Cabibbo-Kobayashi-Maskawa (CKM) matrix and

this controversy inflicts an $\mathcal{O}(15\%)$ uncertainty onto the overall CKM factor $(V_{tb}V_{tq}^*)^2$ of M_{12}^q . This uncertainty drops out from the ratio $\Delta\Gamma_q/\Delta M_q$ in Eq. (1) and also the 4% error from the hadronic matrix element in M_{12}^q largely cancels. The measurements of LHCb [3], CMS [4], ATLAS [5], CDF [6], and DØ [7] combine to

$$\Delta\Gamma_s^{\text{exp}} = (0.082 \pm 0.005) \text{ ps}^{-1} [8], \quad (2)$$

while $\Delta\Gamma_d^{\text{exp}}$ is still consistent with zero. The precise value in Eq. (2) calls for a better SM prediction of $\Delta\Gamma_s$, which is the topic of this Letter. We specify to $q = s$ from now on.

At one-loop level the SM predictions for Γ_{12}^s is calculated from the dispersive part of the $B_s \leftrightarrow \bar{B}_s$ amplitude. One must therefore only consider diagrams with light internal u, c quarks; *i.e.* diagrams with one or two t quarks only contribute to M_{12}^s . To properly accommodate strong interaction effects associated with different energy scales one employs two operator product expansions (OPE). In the first step one matches the SM to an effective theory with $|\Delta B| = 1$ operators [9], where B is the beauty quantum number. The most important operators, *i.e.* those with the largest coefficients, are the current-current operators $Q_{1,2}$ describing tree-level b decays. The effective $|\Delta B| = 1$ hamiltonian is known to next-to-leading (NLO) [10–12] and next-to-next-to-leading order (NNLO) [13–15] of Quantum Chromodynamics (QCD). The OPE employed in the second step of the calculation is the Heavy Quark Expansion (HQE) [16–24] (cf. also [25] for a review), which expresses the $B_s \leftrightarrow \bar{B}_s$ transition amplitude as a series in Λ_{QCD}/m_b , where $\Lambda_{\text{QCD}} \sim 400$ MeV is the fundamental scale of QCD and m_b is the b quark mass. The HQE involves local $|\Delta B| = 2$ operators; to find the corresponding Wilson coefficients one must calculate the $\Delta B = 2$ amplitude in both the $|\Delta B| = 1$ and $|\Delta B| = 2$ theories to the desired order in α_s .

The state of the art is as follows: QCD corrections to Γ_{12}^s are only known for the leading term of the Λ_{QCD}/m_b expansion (“leading power”). These include NLO QCD corrections to the contributions with current-current and

* gerlach.marvin@protonmail.com

† ulrich.nierste@kit.edu

‡ v.shtabovenko@kit.edu

§ matthias.steinhauser@kit.edu

chromomagnetic penguin operators [26–29], the corresponding NNLO corrections (and NLO corrections involving four-quark penguin operators) enhanced by the number N_f of active quark flavours [30–32] as well as NLO results with one current-current and one penguin operator [33] or two penguin operators [34]. The latter paper also presents two-loop results with one or two chromomagnetic penguin operators which are part of the NNLO and $N^3\text{LO}$ contributions. (The four-quark penguin operators Q_{3-6} have Wilson coefficients which are much smaller than those of $Q_{1,2}$ and the chromomagnetic penguin operator contributes with a suppression factor of α_s .) The corrections of Refs. [30] and Refs. [33, 34] have been calculated in an expansion in m_c/m_b to first and second order, respectively. $\Delta\Gamma_s/\Delta M_s$ further involves a well-computed ratio of two hadronic matrix elements [35–37]. The contribution to Γ_{12}^s being sub-leading in Λ_{QCD}/m_b is only known to LO of QCD [38] and the hadronic matrix elements still have large errors [39].

Both the described perturbative contribution and the power-suppressed term have theoretical uncertainties exceeding the experimental error in Eq. (2). In this Letter we present NNLO QCD corrections to the numerically dominant contribution with two current-current operators and reduce the perturbative uncertainty of the leading-power term to the level of the experimental error.

Calculation. To obtain $\Delta\Gamma_s/\Delta M_s$ we use the known two-loop QCD corrections to M_{12}^s from Ref. [11]. It is convenient to decompose Γ_{12}^s according to the CKM structures

$$\Gamma_{12}^s = -(\lambda_c^s)^2 \Gamma_{12}^{cc} - 2\lambda_c^s \lambda_u^s \Gamma_{12}^{uc} - (\lambda_u^s)^2 \Gamma_{12}^{uu}, \quad (3)$$

where $\lambda_a^s = V_{as}^* V_{ab}$ with $a = u, c$. Γ_{12}^s is obtained with the help of a tower of effective theories. In a first step we construct a theory where all degrees of freedom heavier than the bottom quark mass m_b are integrated out and the dynamical degrees of freedom are given by the five lightest quarks and the gluons. We adopt the operator basis of the $|\Delta B| = 1$ theory from Ref. [40]. The matching to the Standard Model happens at the scale $\mu_0 \approx 2m_W \approx m_t(m_t)$. Afterwards, renormalization group running is used to obtain the couplings of the effective operators at the scale μ_1 which is of the order m_b .

In a next step we perform a HQE which allows us to write Γ_{12}^s as an expansion in $1/m_b$. At each order Γ_{12}^s is expressed as a sum of Wilson coefficients multiplying respective operator matrix elements. The latter has to be computed using lattice gauge theory [35] or QCD sum rules [36, 37]. To leading order in the $1/m_b$ expansion we have

$$\Gamma_{12}^{ab} = \frac{G_F^2 m_b^2}{24\pi M_{B_s}} \left[H^{ab}(z) \langle B_s | Q | \bar{B}_s \rangle + \tilde{H}_S^{ab}(z) \langle B_s | \tilde{Q}_S | \bar{B}_s \rangle \right] + \mathcal{O}(\Lambda_{\text{QCD}}/m_b), \quad (4)$$

where $ab \in \{cc, uc, uu\}$. G_F is the Fermi constant and M_{B_s} is the mass of the B_s meson. The main purpose

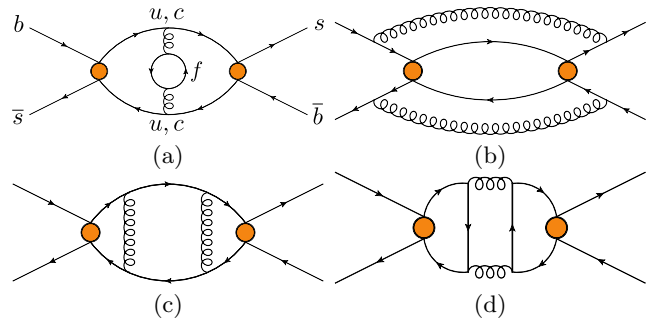


FIG. 1. Representative Feynman diagrams in the $\Delta B = 1$ theory with $f = u, d, s, c, b$. Solid and curly lines represent quarks and gluons, respectively. The (orange) blob indicates an operator insertion.

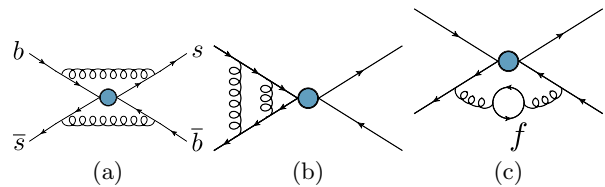


FIG. 2. Representative Feynman diagrams in the $\Delta B = 2$ theory. Solid and curly lines represent quarks and gluons, respectively. The (blue) blob indicates an operator insertion.

of this Letter is the computation of the matching coefficients H^{ab} and \tilde{H}_S^{ab} to next-to-next-to-leading order (NNLO) in the strong coupling constant α_s . They depend on $z = m_c^2/m_b^2$. For the $\Delta B = 1$ theory one distinguishes current-current and penguin operators. At leading and next-to-leading orders the current-current operators provide about 90% of the total contribution to Γ_{12}^{ab} [34]. Thus, in this work we restrict ourselves to the current-current contributions.

For the calculation of the NNLO corrections one has to overcome several challenges. First, it is necessary to perform a three-loop calculation of the amplitude $b\bar{s} \rightarrow \bar{b}s$ in the $\Delta B = 1$ theory. Sample Feynman diagrams are shown in Fig. 1. In total about 20,000 three-loop diagrams have to be considered which requires an automated setup for the computation. In our case the combination of `qgraf` [41], `tapir` [42] and `q2e/exp` [43, 44] turned out to be useful. For the leading term in the HQE we are allowed to set the momentum of the strange quark to zero. Furthermore, we expand in the charm quark mass up to second order,¹ which reduces the integrals to on-shell two-point functions with external momentum $q^2 = m_b^2$. The propagators inside the loop diagrams are either massless or carry the mass m_b . We

¹ Up to this order a naive Taylor expansion of the amplitude is possible except for the fermionic corrections with a closed charm quark loop. These contributions are taken over from Ref. [30, 31].

use FIRE [45] combined with LiteRed [46, 47] to reduce all occurring integrals to 23 genuine three-loop master integrals. For the latter analytic results have been obtained with the help of FeynCalc [48–51], HyperInt [52], PolyLogTools [53] and HyperlogProcedures [54].

On the $\Delta B = 2$ side a two-loop calculation is necessary; sample Feynman diagrams are shown in Fig. 2. From the technical point of view the calculation is significantly simpler. However, in the practical calculation one has to consider three physical and 17 evanescent operators, cf. Ref. [34]). It is necessary to compute the corresponding renormalization constants for the operator mixing up to two-loop order.

The calculation of the $\Delta B = 2$ matrix elements entails a field theoretical subtlety. In fact, in four dimensions there are only two physical operators whereas for the calculation in d dimensions three have to be taken into account. For our calculation it is convenient to choose Q , \tilde{Q}_S and R_0 where (i and j are colour indices)

$$\begin{aligned} Q &= \bar{s}_i \gamma^\mu (1 - \gamma^5) b_i \bar{s}_j \gamma_\mu (1 - \gamma^5) b_j, \\ \tilde{Q}_S &= \bar{s}_i (1 + \gamma^5) b_j \bar{s}_j (1 + \gamma^5) b_i, \end{aligned} \quad (5)$$

and

$$R_0 = Q_S + \alpha_1 \tilde{Q}_S + \frac{1}{2} \alpha_2 Q, \quad (6)$$

with

$$Q_S = \bar{s}_i (1 + \gamma^5) b_i \bar{s}_j (1 + \gamma^5) b_j. \quad (7)$$

Note that at lowest order in α_s we have $\alpha_1 = \alpha_2 = 1$ and the matrix element of R_0 is $1/m_b$ suppressed in four dimensions. At higher orders the quantities α_1 and α_2 are chosen such, that the $1/m_b$ -suppression is maintained. The one-loop corrections are known since more than twenty years [26] and the fermionic two-loop terms are available from Ref. [30]. For the NNLO calculation performed in this Letter the α_s^2 corrections to α_1 and α_2 are needed.

The $1/m_b$ -suppression of R_0 beyond tree-level is manifest only if one is able to distinguish between ultraviolet (UV) and infrared (IR) divergences, e.g., by regularizing the latter using a gluon mass m_g . Otherwise, R_0 develops an unphysical evanescent piece E_{R_0} that scales as m_b^0 [34] and hence must be included into the definition of R_0 to obtain correct matching coefficients. One cannot isolate E_{R_0} from R_0 at the operator level, but one can distinguish evanescent and physical pieces in the matrix elements: We use R_0 from Eq. (6) *including* the finite UV renormalization encoded in α_1 and α_2 in our matching calculation. To this end we have first calculated the linear combination of the renormalized two-loop matrix elements $\langle Q \rangle^{(2)}$, $\langle Q_S \rangle^{(2)}$ and $\langle \tilde{Q}_S \rangle^{(2)}$ as given in Eq. (6). After introducing a gluon mass along the lines of Ref. [55] and using Feynman gauge we observe that each of the individual matrix elements becomes manifestly finite upon UV renormalization. α_1 and α_2 to order α_s^2 are extracted from the requirement that the linear combination must vanish in the limit $m_b \rightarrow \infty$.

$\alpha_s(M_Z) = 0.1179 \pm 0.001$	[58]
$m_c(3 \text{ GeV}) = 0.993 \pm 0.008 \text{ GeV}$	[59]
$m_b(m_b) = 4.163 \pm 0.016 \text{ GeV}$	[59]
$m_t^{\text{pole}} = 172.9 \pm 0.4 \text{ GeV}$	[58]
$M_{B_s} = 5366.88 \text{ MeV}$	[58]
$B_{B_s} = 0.813 \pm 0.034$	[35]
$\tilde{B}'_{S,B_s} = 1.31 \pm 0.09$	[35]
$f_{B_s} = 0.2307 \pm 0.0013 \text{ GeV}$	[60]

TABLE I. Input parameters for the numerical analysis. The matrix elements of Q and \tilde{Q}_S are parametrized in terms of f_{B_s} , B_{B_s} , and \tilde{B}'_{S,B_s} . The values of the quark masses imply $\bar{z} = 0.04956$, $m_b^{\text{pole}} = 4.75 \text{ GeV}$, and $m_b^{\text{PS}} = 4.479 \text{ GeV}$ (for a factorization scale $\mu_f = 2 \text{ GeV}$) at NNLO. Numerical results for the matrix elements of the $1/m_b$ suppressed corrections can be found in Ref. [39].

The matching between the $|\Delta B| = 1$ and $|\Delta B| = 2$ effective theories is conceptually simple in case IR divergences are not regularized dimensionally. In this case the UV renormalization renders amplitudes of both theories manifestly finite, allowing us to take the limit $d \rightarrow 4$, where all matrix elements of evanescent operators vanish. However, for technical reasons we prefer to use $\epsilon = \epsilon_{\text{UV}} = \epsilon_{\text{IR}}$, which simplifies the evaluation of the amplitudes but complicates the matching. Following [56] we need to extend the leading order (LO) matching to $\mathcal{O}(\epsilon^2)$ and the NLO matching to $\mathcal{O}(\epsilon)$ in order to determine the NNLO matching coefficients. Furthermore, we need to determine the matching coefficients of both physical and evanescent operators: Since the UV-renormalized amplitudes still contain IR poles, we must keep all matrix elements of evanescent operators until the very end. A powerful cross check of this procedure is the explicit cancellation of the remaining IR ϵ poles and of the QCD gauge parameter ξ in the matching.

Results. For our numerical analysis we use the input values listed in Tab. I and the $|\Delta B| = 1$ Wilson coefficients from Refs. [13–15] and calculate the running and decoupling of quark masses and α_s with RunDec [57].

In the following we present the NNLO predictions in three different renormalization schemes for the overall factor m_b^2 (cf. Eq. (4)) whereas the quantity z and the strong coupling constant are defined in the $\overline{\text{MS}}$ scheme. The overall factor m_b^2 is defined in the $\overline{\text{MS}}$ scheme, as a pole mass, or as a potential-subtracted (PS) mass [61]. The latter is an example of a so-called threshold mass, with similar properties as the pole mass, but is nevertheless of short-distance nature. $H^{ab}(z)$ and $\tilde{H}_S^{ab}(z)$ are adapted accordingly, so that the scheme dependence of Γ_{12}^s is $\mathcal{O}(\alpha_s^3)$. Several renormalization and matching scales enter the prediction for the width difference. We choose $\mu_0 = 165 \text{ GeV}$ for the matching scale between the SM and the $|\Delta B| = 1$ theory. Varying μ_0 barely affects $\Delta\Gamma_s/\Delta M_s$ and we can keep it fixed. In our nu-

merical analysis we identify the matching scale μ_1 and μ_b and μ_c , the renormalization scales at which \bar{m}_b and \bar{m}_c are defined. We simultaneously vary $\mu_1 = \mu_b = \mu_c$ between 2.1 GeV and 8.4 GeV with a central scale $\mu_1 = 4.2$ GeV. That is, z enters the coefficients as $\bar{z} = (m_c(\mu_1)/m_b(\mu_1))^2$. The $|\Delta B| = 2$ operators are defined at the scale μ_2 which has to be kept fixed, because the μ_2 dependence only cancels in the products of $H^{ab}(z)$ and $\tilde{H}_S^{ab}(z)$ with their respective matrix elements. In our analysis we set $\mu_2 = 4.75$ GeV which is the bottom quark pole mass m_b^{pole} obtained from $m_b(m_b)$ with two-loop accuracy. The terms of order Λ_{QCD}/m_b in Γ_{12}^s are only known to LO, so that the μ_1 -dependence of these terms is non-negligible.

We now discuss the results for $\Delta\Gamma_s/\Delta M_s$. In our three schemes we have

$$\begin{aligned} \frac{\Delta\Gamma_s}{\Delta M_s} &= \left(3.79_{-0.58}^{+0.53} \text{scale} \text{ }_{-0.19}^{+0.09} \text{scale, } 1/m_b \pm 0.11_{B\tilde{B}_S} \right. \\ &\quad \left. \pm 0.78_{1/m_b} \pm 0.05_{\text{input}} \right) \times 10^{-3} \text{ (pole)}, \\ \frac{\Delta\Gamma_s}{\Delta M_s} &= \left(4.33_{-0.44}^{+0.23} \text{scale} \text{ }_{-0.19}^{+0.09} \text{scale, } 1/m_b \pm 0.12_{B\tilde{B}_S} \right. \\ &\quad \left. \pm 0.78_{1/m_b} \pm 0.05_{\text{input}} \right) \times 10^{-3} \text{ (}\overline{\text{MS}}\text{)}, \\ \frac{\Delta\Gamma_s}{\Delta M_s} &= \left(4.20_{-0.39}^{+0.36} \text{scale} \text{ }_{-0.19}^{+0.09} \text{scale, } 1/m_b \pm 0.12_{B\tilde{B}_S} \right. \\ &\quad \left. \pm 0.78_{1/m_b} \pm 0.05_{\text{input}} \right) \times 10^{-3} \text{ (PS)}, \end{aligned} \quad (8)$$

where the subscripts indicate the source of the various uncertainties. The dominant uncertainty comes from the matrix elements of the power-suppressed corrections (“ $1/m_b$ ”) [35, 39] followed by the renormalization scale uncertainty from the variation of μ_1 in the leading-power term (“scale”). The uncertainties from the leading-power bag parameters (“ $B\tilde{B}_S$ ”) and from the scale variation in the $1/m_b$ piece (“scale, $1/m_b$ ”) are much smaller and the variation of the remaining input parameters (“input”) is of minor relevance.

In Fig. 3 we show the dependence of $\Delta\Gamma_s/\Delta M_s$ on the simultaneously varied renormalization scales $\mu_1 = \mu_b = \mu_c$ for the $\overline{\text{MS}}$ and PS schemes. The small contributions involving four-quark penguin operators are only included at NLO in both the NLO and NNLO curves. Dotted, dashed, and solid curves correspond to the LO, NLO, and NNLO results, respectively. In both schemes one observes a clear stabilization of the μ_1 dependence after including higher orders. Furthermore, we observe that the NNLO predictions (solid lines) in both schemes are close together which demonstrates the expected reduction of the scheme dependence. In the $\overline{\text{MS}}$ scheme we observe that the LO and NLO curves intersect close to the central scale. As a consequence the NLO corrections are relatively small and the NNLO contributions are of comparable size. Close to 9 GeV the NNLO contribution is zero and the NLO corrections amount to about +21%. At the same time the NNLO predictions for $\mu_1 = 4.2$ GeV and $\mu_1 = 9$ GeV differ only by +5% and +9% in the $\overline{\text{MS}}$ and PS schemes, respectively. Note that in the $\overline{\text{MS}}$

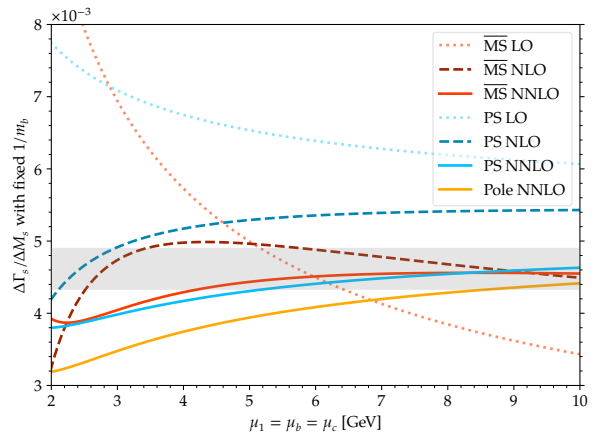


FIG. 3. Renormalization scale dependence at LO, NLO and NNLO for the $\overline{\text{MS}}$ and PS scheme. The scale in the power-suppressed terms is kept fixed. The gray band represents the experimental result.

scheme the scale dependence of the leading-power term drops from $_{-29}^{+0}\%$ at NLO to $_{-10}^{+5}\%$ at NNLO and is now of the same order of magnitude as the $\pm 6\%$ experimental error in Eq. (2). In the PS scheme the scale uncertainty is of the same order of magnitude as in the $\overline{\text{MS}}$ scheme. Note that the scheme dependence inferred from the $\overline{\text{MS}}$ and PS central values in Eq. (8) is only 3%. Eq. (8) clearly shows that one needs better results for the $1/m_b$ matrix elements. A meaningful lattice-continuum matching calls for NLO corrections to the power-suppressed terms, which will further reduce the uncertainty labeled with “scale, $1/m_b$ ”.

For the pole scheme we only show the NNLO prediction in Fig. 3. While we also see a relatively mild dependence on μ_1 , the corresponding solid curve lies significantly below the predictions in the $\overline{\text{MS}}$ and PS schemes. This feature can be traced back to the large two-loop corrections in the relation between the $\overline{\text{MS}}$ and the pole bottom quark mass affecting NNLO contributions as much as the genuine NNLO corrections, underpinning the well-known issues with quark pole masses [62–64]. For this reason we recommend to not use the pole scheme for the prediction of $\Delta\Gamma_s$.

The most precise prediction for $\Delta\Gamma_s$ is obtained from the results in Eq. (8) combined with the experimental result [65] $\Delta M_s^{\text{exp}} = 17.7656 \pm 0.0057 \text{ ps}^{-1}$. Upon adding the various uncertainties in quadrature, symmetrizing the scale dependence and averaging the results from the $\overline{\text{MS}}$ and PS schemes we obtain

$$\Delta\Gamma_s = (0.076 \pm 0.017) \text{ ps}^{-1}. \quad (9)$$

The comparison to Eq. (2) shows that the uncertainty is only about a factor three bigger than from experiment and dominated by the $1/m_b$ corrections.

With our NNLO result for Γ_{12}^q we can also improve the predictions for width difference in the $B_d - \bar{B}_d$ system

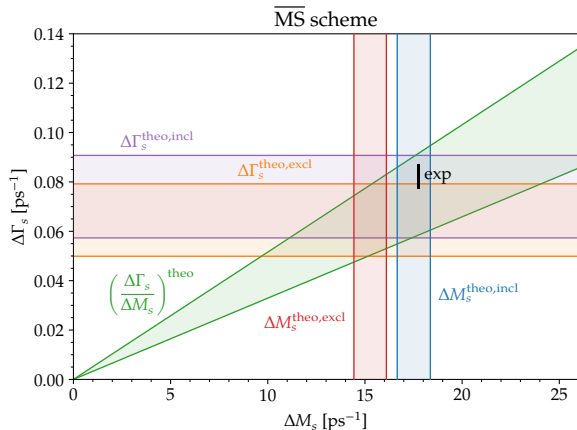


FIG. 4. $\Delta\Gamma_s$ versus ΔM_s . The $|V_{cb}|$ controversy (red vs. blue vertical and orange vs. purple horizontal strips) prevents any conclusion on possible new physics in ΔM_s . A combined analysis of ΔM_s and $\Delta\Gamma_s$ adds important information, because the SM prediction of $\Delta\Gamma_s/\Delta M_s$ (green wedge) is independent of $|V_{cb}|$.

and the CP asymmetries a_{fs}^s and a_{fs}^d in Eq. (1), whose experimental results are still consistent with zero. We postpone this to a future publication [66].

In Fig. 4 we confront our predictions for the ratio $\Delta\Gamma_s/\Delta M_s$ in the $\overline{\text{MS}}$ scheme (green band) with the individual predictions of $\Delta\Gamma_s$ and ΔM_s . The latter are dominated by the uncertainty in the CKM matrix element V_{ts} which is obtained from V_{cb} through CKM unitarity and cancels in the ratio. Fig. 4 illustrates this feature with $|V_{cb}^{\text{incl}}| = 42.16(51)10^{-3}$ from [67] and

$|V_{cb}^{\text{excl}}| = 39.36(68)10^{-3}$ from [68]. The current experimental results for $\Delta\Gamma_s$ and ΔM_s are indicated by the black bar. Once the prediction of $\Delta\Gamma_s/\Delta M_s$ is improved further, it will be possible to test the SM without CKM uncertainty, and with progress on $|V_{cb}|$ one will be able to constrain new physics in ΔM_s and $\Delta\Gamma_s$ individually.

Conclusions. The SM prediction of $\Delta\Gamma_s/\Delta M_s$ based on the long-standing NLO calculation has two sources of uncertainty which exceed the experimental error: the hadronic matrix elements of the power-suppressed operators and the perturbative coefficients, as inferred from the scale and scheme dependences of the calculated result. With the NNLO calculation presented here we have brought the latter uncertainty to the level of the accuracy of the experimental result. For this we had to calculate 20,000 three-loop diagrams and to solve subtle problems related to the interplay of infrared divergences and evanescent operators. We have pointed out that $\Delta\Gamma_s$ adds information to the usual study of ΔM_s , because both quantities probe different new-physics scenarios and $|V_{cb}|$ drops out in the ratio $\Delta\Gamma_s/\Delta M_s$.

Acknowledgements. We thank Artyom Hovhannisyan and Matthew Wingate for useful discussions and we are grateful to Erik Panzer and Oliver Schnetz for helpful advice regarding the calculation of the master integrals and the simplification of the obtained results with `HyperInt` and `HyperLogProcedures`. VS thanks David Broadhurst for enlightening discussions on iterated integrals. This research was supported by the Deutsche Forschungsgemeinschaft (DFG, German Research Foundation) under grant 396021762 — TRR 257 “Particle Physics Phenomenology after the Higgs Discovery”. The Feynman diagrams were drawn with the help of `Axodraw` [69] and `JaxoDraw` [70].

-
- [1] Gilly Elor, Miguel Escudero, and Ann Nelson, “Baryogenesis and Dark Matter from B Mesons,” *Phys. Rev. D* **99**, 035031 (2019), arXiv:1810.00880 [hep-ph].
 - [2] Gonzalo Alonso-Álvarez, Gilly Elor, and Miguel Escudero, “Collider signals of baryogenesis and dark matter from B mesons: A roadmap to discovery,” *Phys. Rev. D* **104**, 035028 (2021), arXiv:2101.02706 [hep-ph].
 - [3] Roel Aaij *et al.* (LHCb), “Updated measurement of time-dependent CP-violating observables in $B_s^0 \rightarrow J/\psi K^+ K^-$ decays,” *Eur. Phys. J. C* **79**, 706 (2019), [Erratum: *Eur.Phys.J.C* 80, 601 (2020)], arXiv:1906.08356 [hep-ex].
 - [4] Albert M Sirunyan *et al.* (CMS), “Measurement of the CP-violating phase ϕ_s in the $B_s^0 \rightarrow J/\psi \phi(1020) \rightarrow \mu^+ \mu^- K^+ K^-$ channel in proton-proton collisions at $\sqrt{s} = 13$ TeV,” *Phys. Lett. B* **816**, 136188 (2021), arXiv:2007.02434 [hep-ex].
 - [5] Georges Aad *et al.* (ATLAS), “Measurement of the CP-violating phase ϕ_s in $B_s^0 \rightarrow J/\psi \phi$ decays in ATLAS at 13 TeV,” *Eur. Phys. J. C* **81**, 342 (2021), arXiv:2001.07115 [hep-ex].
 - [6] T. Aaltonen *et al.* (CDF), “Measurement of the Bottom-Strange Meson Mixing Phase in the Full CDF Data Set,” *Phys. Rev. Lett.* **109**, 171802 (2012), arXiv:1208.2967 [hep-ex].
 - [7] Victor Mukhamedovich Abazov *et al.* (D0), “Measurement of the CP-violating phase $\phi_s^{J/\psi \phi}$ using the flavor-tagged decay $B_s^0 \rightarrow J/\psi \phi$ in 8 fb $^{-1}$ of $p\bar{p}$ collisions,” *Phys. Rev. D* **85**, 032006 (2012), arXiv:1109.3166 [hep-ex].
 - [8] Heavy Flavor Averaging Group (HFLAV), “online update at,” https://hflav-eos.web.cern.ch/hflav-eos/osc/PGD_2020/#DMS.
 - [9] Frederick J. Gilman and Mark B. Wise, “Effective Hamiltonian for Delta $s = 1$ Weak Nonleptonic Decays in the Six Quark Model,” *Phys. Rev. D* **20**, 2392 (1979).
 - [10] Andrzej J. Buras and Peter H. Weisz, “QCD Nonleading Corrections to Weak Decays in Dimensional Regularization and \bar{t} Hooft-Veltman Schemes,” *Nucl. Phys. B* **333**, 66–99 (1990).
 - [11] Andrzej J. Buras, Matthias Jamin, and Peter H. Weisz, “Leading and Next-to-leading QCD Corrections to ϵ Pa-

- parameter and $B^0 - \bar{B}^0$ Mixing in the Presence of a Heavy Top Quark,” Nucl. Phys. B **347**, 491–536 (1990).
- [12] Andrzej J. Buras, Matthias Jamin, M. E. Lautenbacher, and Peter H. Weisz, “Effective Hamiltonians for $\Delta S = 1$ and $\Delta B = 1$ nonleptonic decays beyond the leading logarithmic approximation,” Nucl. Phys. B **370**, 69–104 (1992), [Addendum: Nucl.Phys.B 375, 501 (1992)].
- [13] Martin Gorbahn and Ulrich Haisch, “Effective Hamiltonian for non-leptonic $|\Delta F| = 1$ decays at NNLO in QCD,” Nucl. Phys. B **713**, 291–332 (2005), arXiv:hep-ph/0411071.
- [14] Paolo Gambino, Martin Gorbahn, and Ulrich Haisch, “Anomalous dimension matrix for radiative and rare semileptonic B decays up to three loops,” Nucl. Phys. B **673**, 238–262 (2003), arXiv:hep-ph/0306079.
- [15] Martin Gorbahn, Ulrich Haisch, and Mikolaj Misiak, “Three-loop mixing of dipole operators,” Phys. Rev. Lett. **95**, 102004 (2005), arXiv:hep-ph/0504194.
- [16] Valery A. Khoze and Mikhail A. Shifman, “HEAVY QUARKS,” Sov. Phys. Usp. **26**, 387 (1983).
- [17] Mikhail A. Shifman and M. B. Voloshin, “Preasymptotic Effects in Inclusive Weak Decays of Charmed Particles,” Sov. J. Nucl. Phys. **41**, 120 (1985).
- [18] Valery A. Khoze, Mikhail A. Shifman, N. G. Uraltsev, and M. B. Voloshin, “On Inclusive Hadronic Widths of Beautiful Particles,” Sov. J. Nucl. Phys. **46**, 112 (1987).
- [19] Junegone Chay, Howard Georgi, and Benjamin Grinstein, “Lepton energy distributions in heavy meson decays from QCD,” Phys. Lett. B **247**, 399–405 (1990).
- [20] Ikaros I. Y. Bigi and N. G. Uraltsev, “Gluonic enhancements in non-spectator beauty decays: An Inclusive mirage though an exclusive possibility,” Phys. Lett. B **280**, 271–280 (1992).
- [21] Ikaros I. Y. Bigi, N. G. Uraltsev, and A. I. Vainshtein, “Nonperturbative corrections to inclusive beauty and charm decays: QCD versus phenomenological models,” Phys. Lett. B **293**, 430–436 (1992), [Erratum: Phys.Lett.B 297, 477–477 (1992)], arXiv:hep-ph/9207214.
- [22] Ikaros I. Y. Bigi, Mikhail A. Shifman, N. G. Uraltsev, and Arkady I. Vainshtein, “QCD predictions for lepton spectra in inclusive heavy flavor decays,” Phys. Rev. Lett. **71**, 496–499 (1993), arXiv:hep-ph/9304225.
- [23] B. Blok, L. Koyrakh, Mikhail A. Shifman, and A. I. Vainshtein, “Differential distributions in semileptonic decays of the heavy flavors in QCD,” Phys. Rev. D **49**, 3356 (1994), [Erratum: Phys.Rev.D 50, 3572 (1994)], arXiv:hep-ph/9307247.
- [24] Aneesh V. Manohar and Mark B. Wise, “Inclusive semileptonic B and polarized Lambda(b) decays from QCD,” Phys. Rev. D **49**, 1310–1329 (1994), arXiv:hep-ph/9308246.
- [25] Alexander Lenz, “Lifetimes and heavy quark expansion,” Int. J. Mod. Phys. A **30**, 1543005 (2015), arXiv:1405.3601 [hep-ph].
- [26] M. Beneke, G. Buchalla, C. Greub, A. Lenz, and U. Nierste, “Next-to-leading order QCD corrections to the lifetime difference of B(s) mesons,” Phys. Lett. B **459**, 631–640 (1999), arXiv:hep-ph/9808385.
- [27] M. Ciuchini, E. Franco, V. Lubicz, F. Mescia, and C. Tarantino, “Lifetime differences and CP violation parameters of neutral B mesons at the next-to-leading order in QCD,” JHEP **08**, 031 (2003), arXiv:hep-ph/0308029.
- [28] Martin Beneke, Gerhard Buchalla, Alexander Lenz, and Ulrich Nierste, “CP asymmetry in flavor specific B decays beyond leading logarithms,” Phys. Lett. B **576**, 173–183 (2003), arXiv:hep-ph/0307344.
- [29] Alexander Lenz and Ulrich Nierste, “Theoretical update of $B_s - \bar{B}_s$ mixing,” JHEP **06**, 072 (2007), arXiv:hep-ph/0612167.
- [30] H. M. Asatrian, Artyom Hovhannisyanyan, Ulrich Nierste, and Arsen Yeghiazaryan, “Towards next-to-next-to-leading-log accuracy for the width difference in the $B_s - \bar{B}_s$ system: fermionic contributions to order $(m_c/m_b)^0$ and $(m_c/m_b)^1$,” JHEP **10**, 191 (2017), arXiv:1709.02160 [hep-ph].
- [31] Hrachia M. Asatrian, Hrachya H. Asatryan, Artyom Hovhannisyanyan, Ulrich Nierste, Sergey Tumasyan, and Arsen Yeghiazaryan, “Penguin contribution to the width difference and CP asymmetry in $B_q - \bar{B}_q$ mixing at order $\alpha_s^2 N_f$,” Phys. Rev. D **102**, 033007 (2020), arXiv:2006.13227 [hep-ph].
- [32] Artyom Hovhannisyanyan and Ulrich Nierste, “Addendum to: Towards next-to-next-to-leading-log accuracy for the width difference in the $B_s - \bar{B}_s$ system: fermionic contributions to order $(m_c/m_b)^0$ and $(m_c/m_b)^1$,” (2022), arXiv:2204.11907 [hep-ph].
- [33] Marvin Gerlach, Ulrich Nierste, Vladyslav Shtabovenko, and Matthias Steinhauser, “Two-loop QCD penguin contribution to the width difference in $B_s - \bar{B}_s$ mixing,” JHEP **07**, 043 (2021), arXiv:2106.05979 [hep-ph].
- [34] Marvin Gerlach, Ulrich Nierste, Vladyslav Shtabovenko, and Matthias Steinhauser, “The width difference in $B - \bar{B}$ mixing at order α_s and beyond,” JHEP **04**, 006 (2022), arXiv:2202.12305 [hep-ph].
- [35] R. J. Dowdall, C. T. H. Davies, R. R. Horgan, G. P. Lepage, C. J. Monahan, J. Shigemitsu, and M. Wingate, “Neutral B-meson mixing from full lattice QCD at the physical point,” Phys. Rev. D **100**, 094508 (2019), arXiv:1907.01025 [hep-lat].
- [36] M. Kirk, A. Lenz, and T. Rauh, “Dimension-six matrix elements for meson mixing and lifetimes from sum rules,” JHEP **12**, 068 (2017), [Erratum: JHEP 06, 162 (2020)], arXiv:1711.02100 [hep-ph].
- [37] Daniel King, Alexander Lenz, and Thomas Rauh, “SU(3) breaking effects in B and D meson lifetimes,” (2021), arXiv:2112.03691 [hep-ph].
- [38] M. Beneke, G. Buchalla, and I. Dunietz, “Width Difference in the $B_s - \bar{B}_s$ System,” Phys. Rev. D **54**, 4419–4431 (1996), [Erratum: Phys.Rev.D 83, 119902 (2011)], arXiv:hep-ph/9605259.
- [39] Christine T. H. Davies, Judd Harrison, G. Peter Lepage, Christopher J. Monahan, Junko Shigemitsu, and Matthew Wingate (HPQCD), “Lattice QCD matrix elements for the $B_s^0 - \bar{B}_s^0$ width difference beyond leading order,” Phys. Rev. Lett. **124**, 082001 (2020), arXiv:1910.00970 [hep-lat].
- [40] Konstantin G. Chetyrkin, Mikolaj Misiak, and Manfred Munz, “ $|\Delta F| = 1$ nonleptonic effective Hamiltonian in a simpler scheme,” Nucl. Phys. B **520**, 279–297 (1998), arXiv:hep-ph/9711280.
- [41] Paulo Nogueira, “Automatic Feynman graph generation,” J. Comput. Phys. **105**, 279–289 (1993).
- [42] Marvin Gerlach, Florian Herren, and Martin Lang, “tapir: A tool for topologies, amplitudes, partial fraction decomposition and input for reductions,” (2022), arXiv:2201.05618 [hep-ph].
- [43] R. Harlander, T. Seidensticker, and M. Steinhauser,

- “Complete corrections of Order α_s to the decay of the Z boson into bottom quarks,” *Phys. Lett. B* **426**, 125–132 (1998), arXiv:hep-ph/9712228.
- [44] T. Seidensticker, “Automatic application of successive asymptotic expansions of Feynman diagrams,” in *6th International Workshop on New Computing Techniques in Physics Research: Software Engineering, Artificial Intelligence Neural Nets, Genetic Algorithms, Symbolic Algebra, Automatic Calculation* (1999) arXiv:hep-ph/9905298.
- [45] A. V. Smirnov and F. S. Chuharev, “FIRE6: Feynman Integral REDuction with Modular Arithmetic,” *Comput. Phys. Commun.* **247A**, 106877 (2020), arXiv:1901.07808 [hep-ph].
- [46] R. N. Lee, “Presenting LiteRed: a tool for the Loop INTEgrals REDuction,” (2012), arXiv:1212.2685 [hep-ph].
- [47] Roman N. Lee, “LiteRed 1.4: a powerful tool for reduction of multiloop integrals,” *J. Phys. Conf. Ser.* **523**, 012059 (2014), arXiv:1310.1145 [hep-ph].
- [48] R. Mertig, M. Bohm, and Ansgar Denner, “FEYN CALC: Computer algebraic calculation of Feynman amplitudes,” *Comput. Phys. Commun.* **64**, 345–359 (1991).
- [49] Vladyslav Shtabovenko, Rolf Mertig, and Frederik Orellana, “New Developments in FeynCalc 9.0,” *Comput. Phys. Commun.* **207**, 432–444 (2016), arXiv:1601.01167 [hep-ph].
- [50] Vladyslav Shtabovenko, Rolf Mertig, and Frederik Orellana, “FeynCalc 9.3: New features and improvements,” *Comput. Phys. Commun.* **256**, 107478 (2020), arXiv:2001.04407 [hep-ph].
- [51] Vladyslav Shtabovenko, “FeynCalc goes multiloop,” in *20th International Workshop on Advanced Computing and Analysis Techniques in Physics Research: AI Decoded - Towards Sustainable, Diverse, Performant and Effective Scientific Computing* (2021) arXiv:2112.14132 [hep-ph].
- [52] Erik Panzer, *Feynman integrals and hyperlogarithms*, Ph.D. thesis, Humboldt U. (2015), arXiv:1506.07243 [math-ph].
- [53] Claude Duhr and Falko Dulat, “PolyLogTools — polylogs for the masses,” *JHEP* **08**, 135 (2019), arXiv:1904.07279 [hep-th].
- [54] Oliver Schnetz, “HyperLogProcedures,” <https://www.math.fau.de/person/oliver-schnetz>.
- [55] Konstantin G. Chetyrkin, Mikolaj Misiak, and Manfred Munz, “Beta functions and anomalous dimensions up to three loops,” *Nucl. Phys. B* **518**, 473–494 (1998), arXiv:hep-ph/9711266.
- [56] Marco Ciuchini, E. Franco, V. Lubicz, and F. Mescia, “Next-to-leading order QCD corrections to spectator effects in lifetimes of beauty hadrons,” *Nucl. Phys. B* **625**, 211–238 (2002), arXiv:hep-ph/0110375.
- [57] Florian Herren and Matthias Steinhauser, “Version 3 of RunDec and CRunDec,” *Comput. Phys. Commun.* **224**, 333–345 (2018), arXiv:1703.03751 [hep-ph].
- [58] P. A. Zyla *et al.* (Particle Data Group), “Review of Particle Physics,” *PTEP* **2020**, 083C01 (2020).
- [59] Konstantin G. Chetyrkin, Johann H. Kuhn, Andreas Maier, Philipp Maierhofer, Peter Marquard, Matthias Steinhauser, and Christian Sturm, “Addendum to “Charm and bottom quark masses: An update”,” (2017), 10.1103/PhysRevD.96.116007, [Addendum: *Phys.Rev.D* 96, 116007 (2017)], arXiv:1710.04249 [hep-ph].
- [60] A. Bazavov *et al.*, “B- and D-meson leptonic decay constants from four-flavor lattice QCD,” *Phys. Rev. D* **98**, 074512 (2018), arXiv:1712.09262 [hep-lat].
- [61] M. Beneke, “A Quark mass definition adequate for threshold problems,” *Phys. Lett. B* **434**, 115–125 (1998), arXiv:hep-ph/9804241.
- [62] Ikaros I. Y. Bigi, Mikhail A. Shifman, N. G. Uraltsev, and A. I. Vainshtein, “The Pole mass of the heavy quark. Perturbation theory and beyond,” *Phys. Rev. D* **50**, 2234–2246 (1994), arXiv:hep-ph/9402360.
- [63] M. Beneke and Vladimir M. Braun, “Heavy quark effective theory beyond perturbation theory: Renormalons, the pole mass and the residual mass term,” *Nucl. Phys. B* **426**, 301–343 (1994), arXiv:hep-ph/9402364.
- [64] Martin Beneke, “Pole mass renormalon and its ramifications,” *Eur. Phys. J. ST* **230**, 2565–2579 (2021), arXiv:2108.04861 [hep-ph].
- [65] R. Aaij *et al.* (LHCb), “Precise determination of the $B_s^0-\bar{B}_s^0$ oscillation frequency,” *Nature Phys.* **18**, 1–5 (2022), arXiv:2104.04421 [hep-ex].
- [66] Marvin Gerlach, Ulrich Nierste, Vladyslav Shtabovenko, and Matthias Steinhauser, “Next-to-next-to-leading order QCD corrections to the B-meson mixing,” in preparation.
- [67] Marzia Bordone, Bernat Capdevila, and Paolo Gambino, “Three loop calculations and inclusive Vcb,” *Phys. Lett. B* **822**, 136679 (2021), arXiv:2107.00604 [hep-ph].
- [68] Y. Aoki *et al.*, “FLAG Review 2021,” (2021), arXiv:2111.09849 [hep-lat].
- [69] J. A. M. Vermaseren, “Axodraw,” *Comput. Phys. Commun.* **83**, 45–58 (1994).
- [70] D. Binosi and L. Theussl, “JaxoDraw: A Graphical user interface for drawing Feynman diagrams,” *Comput. Phys. Commun.* **161**, 76–86 (2004), arXiv:hep-ph/0309015.